Acta Cryst. (1977). A33, 137–142

Determination of Strain Distributions from X-ray Bragg Reflexion by Silicon Single Crystals

BY AKIRA FUKUHARA AND YUKIO TAKANO

Central Research Laboratory, Hitachi Ltd., Kokubunji, Tokyo, Japan

(*Received* 16 *January* 1976; *accepted* 12 *July* 1976)

Accurate determination of strain distributions normal to the crystal surface is attempted through best-fitting of intensity profiles recorded with a double-crystal diffractometer and corresponding theoretical curves computed within the frame of the dynamical diffraction theory. The strain distributions are assumed to be one-dimensional and their functional forms are supposed from the sample preparation process. The fits are quite satisfactory for three samples prepared by boron diffusion, phosphorus diffusion and epitaxic growth with germanium doping. For samples containing boron and phosphorus, sheet-resistivity measurements combined with anodic oxidation showed diffusant distributions which were reasonably proportional to the strain distributions assumed above. Ratios of strain to impurity concentration measured here are *ca* 40% larger than those defined for uniform doping; simple elasticity considerations give an interpretation of this fact and the factor can be expressed in terms of stiffness constants.

1. Introduction

Crystal distortions have been widely studied through X-ray diffraction especially in connexion with the investigation of materials for solid-state devices. Impurity diffusion, epitaxic growth, or ion implantation introduce various amounts of lattice distortion near the surface of crystal plates. The distortion causes modifications in the intensity profile of Bragg-case diffraction from wafers processed in these ways, *i.e.* the appearance of additional peaks, change in height and/or width of peaks, *etc.* (Cohen, 1967; Burgeat & Taupin, 1968; Burgeat & Colella, 1969; Yagi, Miyamoto & Nishizawa, 1970).

Burgeat & Taupin (1968) and Burgeat & Colella (1969) have demonstrated strain estimation from experimental intensity profiles by the dynamical theory of X-ray diffraction for distorted crystal lattices (Takagi, 1962, 1969; Taupin, 1964). Once the reliability and accuracy of such a method is confirmed, this non-destructive measurement can be applied to quantitative analyses which will be of practical use in the understanding of phenomena related to lattice distortion.

In the present experiment with a double-crystal diffractometer in parallel setting, particular care was exercised, for the sake of accuracy and clarity in the analysis, as follows. (1) The 333 reflexion of Cu $K\alpha$ X-radiation was chosen, of which the Bragg angle is near 45°, so that the polarization state involved should be an almost pure σ-state. (2) The angular spread of the X-ray beam incident on the sample crystal was made as small as 0·25 seconds* by an asymmetric 511 reflexion of the first crystal in order to reduce the degradation of rocking curves due to the beam spread (Renninger, 1961; Kohra, 1962). (3) The analyses were performed also for the samples for which the impurity distributions with depth were measured independently of the distortion analyses to provide a clear discussion about the relation between the impurity concentration and the induced strains.

The purpose of this report is to show the improvements in the strain analyses resulting from the considerations stated above and to propose that analysis of this kind deserves practical applications.

* This value corresponds to about one eighth of the angular width of the rocking curve of symmetric 511 or 333 reflexion.

2. Theoretical

Computations of Bragg-reflexion intensities, which must be performed more or less numerically, are greatly simplified under the following conditions: (1) the crystal plate can be regarded as flat over the irradiated area, (2) the lattice is distorted only in the direction of the surface normal; that is, only a strain component e_{zz} is different from zero in a Cartesian coordinate system where z is taken as parallel to the normal.

These conditions are closely related to each other and both are satisfied when the sample substrate is thick enough not to allow stress relief by buckling.

As for polarization of X-rays only the σ-state will be considered for the sake of simplicity. It suffices here to describe the procedure only roughly, as the final results prove substantially the same as those given previously by Burgeat & Taupin (1968).

Initially, a strain distribution is presumed from the process of sample preparation and is given as a function of depth z. Then for a local (distorted) crystal structure at an arbitrary z the eigenvalue problem shown below is solved in the same way as for a perfect crystal:

$$\begin{pmatrix} k_\perp^2+k_\parallel^2-K^2(1+\varphi_0) & -K^2\varphi_{\bar{h}} \\ -K^2\varphi_h & (k_\perp+h_\perp)^2+(\mathbf{k}_\parallel+\mathbf{h}_\parallel)^2-K^2(1+\varphi_0) \end{pmatrix} \begin{pmatrix} 1 \\ R \end{pmatrix} = 0\,, \qquad (1)$$

where the φ's are Fourier coefficients of the polarizability multiplied by 4π, K and k are 2π times the wavenumber of X-rays in vacuo and in the crystal respectively, $\mathbf{h}$ is the relevant reciprocal vector, R the ratio of the amplitude of the reflected wave to that of the transmitted wave in the 'local' structure, and subscripts $\parallel$ and $\perp$ stand for vector components parallel and perpendicular to the crystal surface respectively.

The quantities $k_\perp$ and R are to be determined simultaneously. The vectors $\mathbf{k}_\parallel$ and $\mathbf{h}_\parallel$ are given independently of z by the geometry of the X-ray incidence, the surface and the crystal orientation, while only $h_\perp$ depends on z. Among solutions thus obtained, two physically significant ones that have $k_\perp$ values near $K_\perp$ are chosen and used with superscripts 1 and 2 in the following equation for 'local reflectivity', S:

$$\frac{\mathrm{d}S}{\mathrm{d}z} = -i\frac{k_\perp^{(1)}-k_\perp^{(2)}}{R^{(1)}-R^{(2)}}(R^{(1)}-S)\,(R^{(2)}-S)\,. \qquad (2)$$

When $k_\perp$ and R are constant, this equation can be solved analytically to give the well known results for perfect crystals. For the present purpose, however, the equation must be numerically integrated under the boundary condition that only an out-going wave exists outside of the bottom surface. When the crystal plate is very thick, the condition may be such that S approaches $R^{(1)}$ asymptotically, a solution of (1) having a damped form towards larger z.

Ratio $I(\theta_0)$ of the reflected to the incident intensity is now obtained as

$$I(\theta_0) = |S(z=0)|^2\,(\cos\theta_0/\cos\theta_h)\,, \qquad (3)$$

where the incident and the reflected beams incline at angles θ_0 and θ_h respectively to the entrance surface. The procedure from (1) to (3) is repeated for θ_0 values around the Bragg condition to predict the intensity profile or rocking curve of the sample crystal.

3. Experimental

When a crystal is uniformly doped the proportion of the coefficient of strain (relative change in lattice spacing) to impurity concentration is well defined, as will be described later, and its value will be of fundamental importance in quantitative discussions. Coefficients thus defined have been measured for boron and phosphorus in silicon by a method (Takano & Maki, 1973) devised by one of the present authors for the precise determination of the difference in the Bragg angle between a sample and a reference crystal. The experimental results are illustrated in Fig. 1.

When the impurity distribution in a sample is not uniform, the rocking curve from the sample shows a complicated profile. Three such samples, (111) wafers of silicon with different impurities, were tested with a

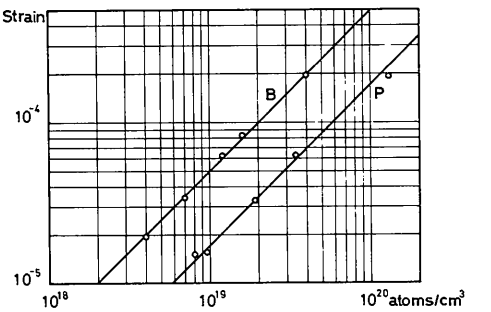

Fig. 1. Lattice strain *versus* impurity concentration for uniform doping in silicon. The abscissa is estimated from resistivity measurements.

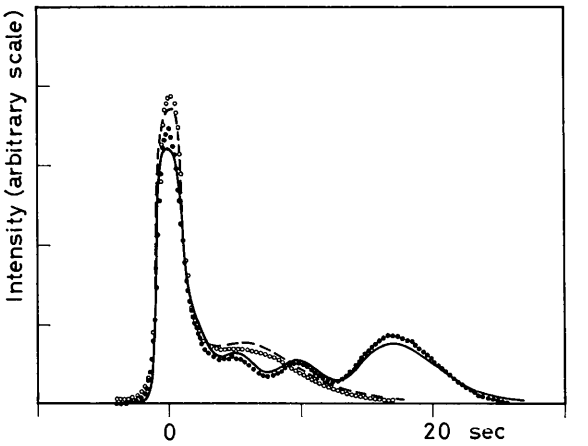

Fig. 2. Rocking curves of a silicon crystal including boron. Unetched surface: experimental ●●●, theoretical ——; etched surface: experimental ○○○, theoretical — —.

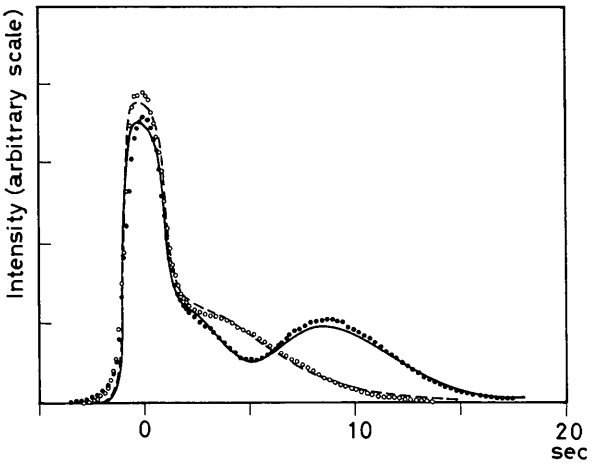

Fig. 3. Rocking curves of a silicon crystal including phosphorus.

double-crystal diffractometer of parallel setting, in which an asymmetric 511 reflexion for collimation reduced the horizontal angular divergence of X-rays to 0·25 seconds and the long distance between the source and the sample limited the vertical divergence to *ca* 4·2 minutes. The combination of Cu $K\alpha$ X-rays and 333 Bragg reflexions in the samples was chosen so that the Bragg angle would be near 45° and hence only one polarization state should be involved. The choice stated here makes the interpretation of experimental results simpler and clearer, but was not properly considered in some previously reported experiments (Cohen, 1967; Burgeat & Taupin, 1968; Burgeat & Colella, 1969; Yagi, Miyamoto & Nishizawa, 1970).

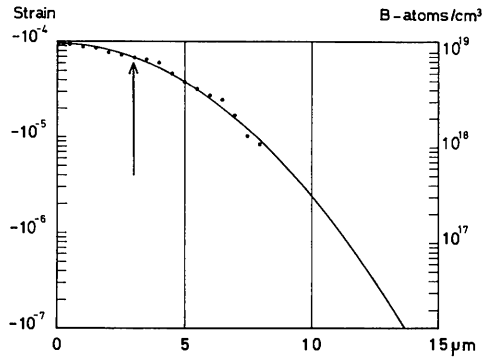

Fig. 4. Proportionality between the strain (—) assumed for the theoretical curve in Fig. 2 and the boron distribution (· · ·). The arrow shows the assumed thickness of the removed layer.

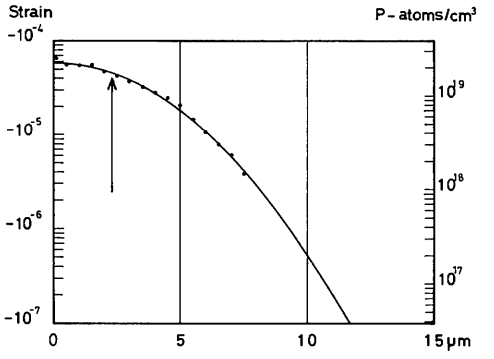

Fig. 5. Proportionality between the strain (—) assumed for Fig. 3 and the phosphorus distribution (· · ·).

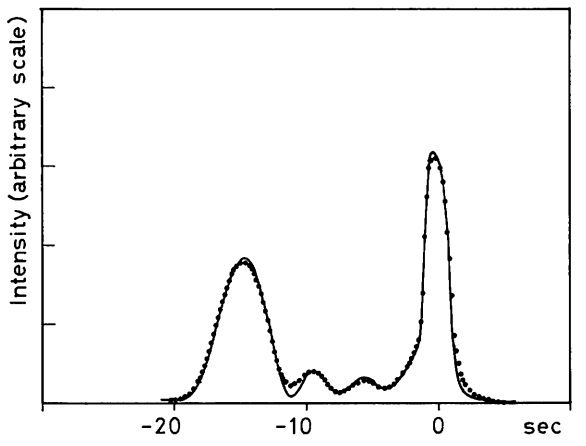

Fig. 6. Computed (—) and experimental (· · ·) rocking curves of a silicon crystal with an epitaxic layer doped with germanium.

(1) The first and second samples were 2 mm-thick, (111) wafers annealed in a nitrogen atmosphere after being subjected to a source of solid diffusant, boron or phosphorus. No dislocation was observed in them by the Lang method. A part of the surface of each sample was chemically etched off; the thickness of the removed layers was measured mechanically as 3·5 and 2·3 μm respectively. The rocking curves of normal and etched surfaces of both samples are reproduced in Figs. 2 and 3.

During the computational procedure described in the previous section, theoretical rocking curves were worked out for strain distributions of Gaussian type which are consistent with the sample preparation process (Runyan, 1965), and adjusted so as to fit the experimental curves. Similar procedures were also followed for the data of the etched-off surfaces with the etching thickness as a new, free parameter to be adjusted. Figs. 2 and 3 show the final fit so far obtained, and the strain distributions assumed to give the final theoretical curves are shown in Figs. 4 and 5.

Repetition of sheet-resistivity measurements combined with anodic oxidation (Tannenbaum, 1961) was subsequently applied to these two samples in order to estimate the impurity distributions, which are also shown in Figs. 4 and 5.

(2) The third sample contains a germanium-doped epitaxic layer grown on a 2 mm-thick (111) substrate; the layer was grown for 6 min at 1190°C and is some 7 μm thick. The dots in Fig. 6 show the rocking curve obtained from this sample.

4. Discussion

The introduction of impurity atoms into a pure-matrix crystal brings about lattice imperfections, among which elastic strain appears at first in proportion to the impurity concentration, and then defects such as dislocations occur to relax the strain when the latter exceeds a critical value. There can be no doubt as to the proportionality of the strain well below the critical value, but care should be exercised when the proportionality coefficient is to be quantitatively discussed. A local strain value depends not only on the impurity concentration at the location itself but also on the strain distribution in its vicinity.

To start with a simple concept, let us consider a crystal of cubic structure uniformly doped with an impurity. No shearing strain appears and all other strain components must show the same uniform value. The

proportionality coefficient is well defined in such situations.

Next let us proceed to strains due to an impurity distributed along the depth z in a parallel-plate crystal of thickness d. Consider a 'free' strain $e_0(z)$, *i.e.* the product of the concentration and the proportionality coefficient defined for uniform distributions. Actual strain differs from $e_0(z)$ and the difference gives rise to elastic stresses; the optimum condition of the whole elastic energy determines the actual distribution of stress and strain. To discuss the generation of dislocations, Prussin (1961) and Czaya (1966) used a relation between the stress distribution and the impurity concentration analogous to the stress variation under a temperature distribution derived by Timoshenko (1934). The assumption that the concentration distributions are one-dimensional is common both to their discussions and the present report, but in addition they had regarded the crystal as an isotropic medium. At this point a more rigorous relation will be introduced as follows.

For the sake of simplicity, only those crystal plates are considered of which the surface normal is parallel to the axis of high symmetry, *i.e.* $z \parallel \langle 001\rangle$ or $\langle 111\rangle$, and which are flat, or bent in a spherical shell. Let e_z and e_t denote elongations parallel and perpendicular to z respectively. Other strain components do not appear under the assumptions made.

The variation calculus leads to the following expressions:

$$\left.\begin{aligned} e_z(z) &= (1+2a)e_0(z) - 2ae_t(z) && z \parallel \langle 001\rangle, \\ e_z(z) &= [3(1+2a)e_0(z) - 2(1+2a-2b)e_t(z)]/(1+2a+4b) && z \parallel \langle 111\rangle, \end{aligned}\right\} \tag{4}$$

$$\left.\begin{aligned} e_t(z) &= \bar{e}_0 + (z-d/2)/r \\ 1/r &= 6(2z-d)e_0/d^2 \end{aligned}\right\} \text{ for both cases,} \tag{5}$$

where the numerical factors a and b are defined in terms of elastic stiffness coefficients as $a = C_{12}/C_{11}$ and $b = C_{44}/C_{11}$. In the equations, r is the radius of curvature of the plate, and the barred symbols stand for values averaged with respect to depth. We can ignore e_t for the thick samples treated in the previous section. Eventually the proportion coefficient in question is multiplied by the numerical factor determined only from the elastic property due to the non-uniform impurity distribution:

$$\begin{aligned} 1+2a \quad & (=1{\cdot}77 \text{ for Si}) \quad z \parallel \langle 001\rangle, \\ 3(1+2a)/(1+2a+4b) \quad & (=1{\cdot}44 \text{ for Si}) \quad z \parallel \langle 111\rangle. \end{aligned} \tag{6}$$

Now let us examine the data of the first and second samples in the previous section following the above discussion. Firstly, proportionality between the strain and the impurity concentration holds tolerably well, even when they are not uniform, as seen in Figs. 4 and 5. From these one can estimate the proportionality constants as $7{\cdot}2 \times 10^{-24}$ and $2{\cdot}4 \times 10^{-24}$ cm^3 atom^{-1} respectively.

We have already seen from the data illustrated in Fig. 1 that the constants for uniform distributions are $(5{\cdot}00 \pm 0{\cdot}16) \times 10^{-24}$ and $(1{\cdot}72 \pm 0{\cdot}15) \times 10^{-24}$ cm^3 atom^{-1} respectively. Thus, the multiplication factor resulting from non-uniform distributions is 1·4 for both cases. This agrees well with the value given by (6); a fact which supports the validity of the physical picture leading to (6).

The slight but systematic discrepancy shown in Fig. 2 seems to reveal the fact that the actual strain falls off a little more steeply than a Gaussian function expresses. This could not be confirmed from the measured impurity distribution owing to experimental ambiguities.

The impurity distribution in the third sample assumes the following functional form (Runyan, 1965) for a growth time t, if the growth rate g, diffusion coefficient D of the impurity, and the impurity concentration at the surface are all perfectly constant with time:

$$f(z) = [f(0)/\sqrt{\pi}]\left[\operatorname{erfc}\left(\frac{z-z_s}{z_d}\right) + \operatorname{erfc}\left(\frac{z+z_s}{z_d}\right)\exp\left(-\frac{4zz_s}{z_d^2}\right)\right], \tag{7}$$

where

$$z_s = gt, \quad z_d = 2\sqrt{(Dt)}, \quad \operatorname{erfc}(x) = \int_x^\infty \mathrm{d}y \exp(-y^2).$$

The strain distribution must be proportional to expression (7).

Since germanium diffuses little in silicon the concentration profile may behave like a step function of z as deduced from (7) with a small z_d. Some preliminary computations have shown that a strain distribution of sharp step-function form does not explain the two minor maxima observed in the recorded rocking curve.

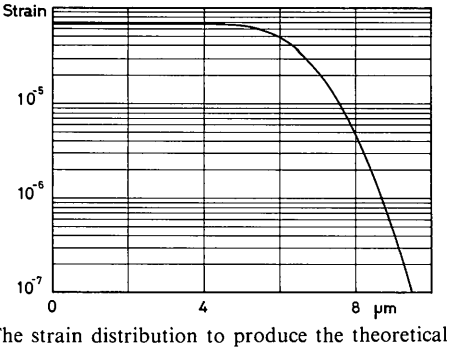

Fig. 7. The strain distribution to produce the theoretical curve in Fig. 6.

Eventually $f(0)$, z_s and z_d were regarded as free parameters to adjust the theoretical curve, which resulted in a satisfactory fit to the experimental curve as shown in Fig. 6. The final strain profile is shown in Fig. 7.

A measurement of D (Namba, 1972) suggests the z_d value in the present case should be 0·006 μm, exceedingly small compared with the adjusted value 1·5 μm. This discrepancy seems to arise from the fact that the epitaxic growth in the sample did not start with an ideal abruptness nor proceed with perfect constancy of g and $f(0)$: thus the boundary must have been blurred, which corresponds effectively to a larger z_d.

As for Figs. 2, 3 and 6 the fit is much better than the present authors expected and seems encouraging for analyses of strain by this method. Physical meanings of intensity profiles have been confirmed through 'computer experiments' and are summarized as follows.

Typical intensity profiles consist of a sharp peak coming from the thick substrate and a broader peak from the distorted surface layer accompanied by minor subsidiary maxima. Theoretically, the subsidiaries may appear on both sides of the broad peak or hump, but they have always been observed between the sharp and the broad peaks; the reason is that the subsidiaries are greatly enhanced by the interference between the (tails of) the two peaks. When the distorted surface layer becomes thinner, the minor maxima are more widely spaced (in angle) and the hump gets smaller and broader. The maxima themselves are due to the finite thickness of the surface layer, obviously in the way that '*Pendellösung*' phenomena (Batterman & Hildebrandt, 1968; Renninger, 1968; Nakayama, Hashizume & Kohra, 1970) are due to finite thicknesses of crystal plates. The maxima disappear and the hump combines with the sharp peak into a composite peak when the distortion or thickness of the surface layer is quite small. In addition, the more diffuse the boundary between the distorted layer and the substrate is, the stronger the intensity between the sharp peak and the hump becomes.

The knowledge of the characteristics of intensity profiles described here is of practical use in interpreting recorded profiles and estimating strain distributions. It should also be emphasized here that quantitative conclusions must be drawn from numerical computations as done in this report; otherwise a certain error will result in the strain estimate, described as follows. Lattice strain has often been evaluated from the angular spacing of double peaks in an intensity profile and the formula $\Delta d/d = -\Delta\theta \cot\theta_B$ (Cohen, 1967; Yagi, Miyamoto & Nishizawa, 1970; Miyamoto, Kuroda & Yoshida, 1973; Nishizawa, Terasaki, Yagi & Miyamoto, 1975). If the estimated strain is intended as the value at the surface, this simple method gives an underestimate of the value of a strain distribution descreasing with depth; such an estimate for the example of Fig. 3 includes an error of 33% when compared with the value in Fig. 5. Peak spacing is not the only information we can acquire from an intensity profile and the profile should be utilized as a whole to derive a complete distribution of lattice strain.

5. Conclusion

Three examples examined in this report show unexpectedly good agreement between experimental and computed diffraction profiles, owing to the condition that the angular spread of the incident X-rays was made small by asymmetric reflexion of the collimator crystal and reflexion of the Bragg angle near 45° was adopted, and to the assumed form of strain distribution being appropriate.

For two samples the distributions of the impurities boron and phosphorus were estimated through resistivity measurements, and their dependences on depth were found to be similar to the strain distribution assumed for computing the diffraction profile. The ratio of strain to impurity concentration thus obtained for (111) wafers is some 1·4 times as large as the ratio of lattice-parameter change to impurity density in uniform doping in the two cases of boron and phosphorus; this multiplying factor due to non-uniformity of distribution can be explained from elasticity considerations.

The facts stated above suggest future quantitative strain analyses by X-ray diffraction; *e.g.* the application to non-destructive investigations of impurity distributions, measurement of diffusion constants, *etc.* within the limits of the proportionality between strain and impurity concentration. It should be noted in our examples that electric-resistivity measurement is of no use in the detection of impurity germanium nor is activation analysis of use in detecting boron atoms diffused into silicon.

Thinner surface layers, say some 1 μm thick, may be more interesting objects of this analysis from the viewpoint of application to electronic devices. This is being studied by the present authors to utilize the asymmetric Bragg reflexions for such analyses and the results will be reported in the near future.

The authors would like to express their sincere gratitude to Mr M. Maki for valuable discussions and continual encouragement. They also thank Mr M. Namba for measuring the diffusion constant of Ge and preparing samples by impurity diffusion and Mr K. Saida for preparing the epitaxic sample.

References

BATTERMAN, B. W. & HILDEBRANDT, G. (1968). *Acta Cryst.* A **24**, 150–157.

BURGEAT, J. & COLELLA, R. (1969). *J. Appl. Phys.* **40**, 3505–3509.

BURGEAT, J. & TAUPIN, D. (1968). *Acta Cryst.* A **24**, 99–102.

COHEN, B. G. (1967). *Solid-State Electron.* **10**, 33–37.

CZAYA, W. (1966). *J. Appl. Phys.* **37**, 3441–3446.

KOHRA, K. (1962). *J. Phys. Soc. Japan*, **17**, 589.
MIYAMOTO, N., KURODA, E. & YOSHIDA, S. (1973). *Proc. 5th Conf. Solid State Devices, Tokyo*: *Jap. J. Appl. Phys. Suppl.* (1974). **43**, 408–414.
NAKAYAMA, K., HASHIZUME, H. & KOHRA, K. (1970). *J. Phys. Soc. Japan*, **30**, 893.
NAMBA, N. (1972). Private communication.
NISHIZAWA, J., TERASAKI, T., YAGI, K. & MIYAMOTO, N. (1975). *J. Electrochem. Soc.* **122**, 664–669.
PRUSSIN, S. (1961). *J. Appl. Phys.* **32**, 1876–1881.
RENNINGER, M. (1961). *Z. Naturforsch.* **16***a*, 1110.
RENNINGER, M. (1968). *Acta Cryst.* A**24**, 143–149.
RUNYAN, W. R. (1965). *Silicon Semiconductor Technology*, pp. 122–127. New York: McGraw-Hill.
TAKAGI, S. (1962). *Acta Cryst.* **15**, 1311–1313.
TAKAGI, S. (1969). *J. Phys. Soc. Japan*, **26**, 1239–1253.
TAKANO, Y. & MAKI, M. (1973). *Semiconductor Silicon* 1973, pp. 469–477. New Jersey: The Electrochemical Society.
TANNENBAUM, E. (1961). *Solid-State Electron.* **2**, 123–132.
TAUPIN, D. (1964). *Bull. Soc. Fr. Minér. Crist.* **87**, 469–511.
TIMOSHENKO, S. (1934). *Theory of Elasticity*, 1st ed. p. 203. New York: McGraw-Hill.
YAGI, K., MIYAMOTO, N. & NISHIZAWA, J. (1970). *Jap. J. Appl. Phys.* **9**, 246–254.

Acta Cryst. (1977). A**33**, 142–145

Neutron Powder Diffraction and Constrained Refinement. The Structures of *p*-Dibromo- and *p*-Diiodotetrafluorobenzene

BY G. S. PAWLEY AND G. A. MACKENZIE
Physics Department, Edinburgh University, EH9 3JZ, Scotland

AND O. W. DIETRICH
Physics Department, AEK Risø, Roskilde 4000, *Denmark*

(*Received* 11 *June* 1976; *accepted* 4 *July* 1976)

The first use of a new program, *EDINP*, is reported. This program allows the constrained refinement of molecules in a crystal structure with neutron diffraction powder data. The structures of *p*-$C_6F_4Br_2$ and *p*-$C_6F_4I_2$ are determined by packing considerations and then refined with *EDINP*. Refinement is stable and rapid, and the data are sufficiently accurate to allow the choice of the correct minimum in the presence of a number of false minima. A fuller report on *EDINP* is planned.

Introduction

The purpose of this study is to investigate the potential of the neutron powder diffraction method as applied to molecular crystals. The structures most commonly found in molecular systems tend to be of low symmetry, predominantly monoclinic, and with fairly large unit cells. This gives rise to a large number of powder diffraction peaks, even at low angles, which overlap each other considerably. Thermal motion causes a more rapid fall-off in intensity with scattering angle than is observed with harder crystals. In consequence, studies of such systems must rely considerably on the restricted range of low-order peaks in the diffraction pattern.

It is well known that in single-crystal structure refinements it is impossible to vary more parameters than there are observations. The problem – how many structure parameters can be varied with a given powder scan? – is not yet solved, and the solution may have to be based on experience. However, it will always be true to say that success is more likely if the number of variable parameters is sensibly reduced, and in the case of molecular systems, where the number of atoms may be very large, such a reduction can be made by the use of constraints (Pawley, 1972*a*). This imposes a restriction on the type of problem that can be tackled, as the refinement of a completely unknown structure with a large number of atoms is (at present at least) out of the question.

Phase transitions, brought about by changing pressure or temperature, are common in molecular systems, and the study of such systems can give information about the intermolecular forces. In most phase transitions no chemical reaction takes place, and therefore it can be assumed that no change other than a steric rearrangement has taken place in the molecule. In constraining a molecule so that it retains its integrity this fact can be used to advantage.

The structures chosen for study are very similar to *p*-dichlorobenzene which shows an interesting phase transition [Housty & Clastre (1957); Reynolds, Kjems & White (1972)]. They are *p*-dibromo- and *p*-diiodotetrafluorobenzene, and DTA shows the latter to have a phase change at approximately 85 °C. Their melting points are approximately 80 and 107 °C respectively. Only the room-temperature phases have been thoroughly studied, and powder diffraction scans of both samples were measured at 150 and 300 K on the TAS II spectrometer at AEK Risø. Neutrons of